The effect of carbon dioxide dissolved in water on some properties of Carboxymethyl cellulose and Polyanionic cellulose used in the oil field

Najla Ali Elgheryani
Department of Physics, College of Education, University of Benghazi, Benghazi, Libya.
*Corresponding author: nagla.elgerani@uob.edu.ly

Submission data: 29 .11.2024 Acceptance data: 28. 1 .2025 Electronic publishing data: 30.1.2025

Abstract: This paper investigates the impact of atmospheric carbon dioxide(CO_2) on the electrical properties, viscosity, and surface tension of Carboxymethyl cellulose (CMCHV) and Polyanionic cellulose (PACLV) when dissolved in water used for oil extraction. The research reveals that as carbon dioxide concentrations increase, the conductivity, viscosity, and surface tension of these substances also increase, albeit to varying extents. The findings suggest that the presence of carbon dioxide in the atmosphere can alter the physical properties of CMCHV and PACLV when they are dissolved in water used for oil extraction in oilfields and wells. This is significant because these substances are commonly used in solid-laden and water-based drilling fluids, where high viscosity can impede the filtration rate of many water-based drilling fluids. Ideally, these substances should have low viscosity. The results of this study can be used to modify the physical properties of CMCHV and PACLV, particularly their viscosity, to mitigate the effects of carbon dioxide on their behavior

Keywords: Carbon dioxide, electrical properties, viscosity, surface tension, Carboxymethyl cellulose, Polyanionic cellulose

Introduction:

Carbon dioxide is a vital component of our environment, influencing atmospheric dynamics, contributing to global warming, and playing a role in subsurface geochemistry [1].

Since the 1960s, the concentration of carbon dioxide in the atmosphere has been steadily increasing. The use of carbon dioxide can significantly enhance the efficiency of in-situ oil recovery and hydraulic fracturing. However, the viscosity of carbon dioxide is a crucial factor in these processes, as it affects the efficiency of carbon dioxide sequestration in brine layers, carbon dioxide recovery, and hydraulic fracturing. Under subsurface conditions, carbon dioxide exhibits a liquid-like density but a gas-like viscosity, which can make it ineffective for in-situ oil recovery due to its low sweep efficiency. Furthermore, carbon dioxide can cause premature breakouts due to fluid displacement in cores and injection in large-scale fields [2]. At normal temperature and pressure, carbon dioxide exists as a gas, but its physical state changes with temperature and pressure. At low temperatures, carbon dioxide becomes a solid, and when heated, it sublimates directly into vapour if the pressure is less than 5.1 bar [3].

Carboxymethyl cellulose is a promising cellulose derivative with unique surface properties, mechanical strength, and viscoelastic properties. Its availability, abundance of raw materials, and low-cost synthesis process make it an attractive material for various applications, including food, paper, textile, pharmaceutical, biomedical engineering, wastewater treatment, power generation, and energy storage production [4]. Despite its numerous uses in various fields, including the petroleum industry, there is limited research on the role of carboxymethyl cellulose in the oil and gas field [5].

Polyanionic cellulose is commonly used as a viscosity-increasing agent for drilling fluids in oil drilling operations. It is also used as a substitute for drilling fluid when dissolved in distilled water in cuttings transfer studies or other multiphase flow studies relevant to the oil and gas industry. Cuttings transfer refers to the process of properly purging solids removed from an oil well [6].

Theoretical Models

The electrical properties

The electric current density (J) is determined by the product of the charge intensity, the number density, and the drift velocity of the charge carriers. In an Ohmic conductor, the electric field intensity is directly related to the drift velocity of the electric charge carriers [7]. This relationship arises from the balance between the deceleration caused by collisions between the charges and the grid, and the acceleration resulting from the electric field (E) [8]. When the acceleration due to the electric field and the deceleration due to collisions between the charges and the grid are in equilibrium, the drift velocity and the electric field intensity become proportional. This proportionality gives rise to Ohm's microscopic law, which describes the relationship between the current density and the electric field. According to this law, the current density is directly proportional to the electric field, as expressed by a fundamental

equation(1) that governs the behavior of electric currents in conductors [9, 10].

$$J = \sigma_{dc} E \quad (1)$$

Where:

$$J = \frac{I}{A} \quad (2)$$

$$\sigma_{dc} = \frac{1}{\rho_{dc}}, \qquad \rho_{dc} = \frac{R\,A}{L} \quad (3)$$

And I is the intensity of the direct current, A is the surface area of the sample, σ_{dc} is the electrical conductivity (measured in Ω^{-1}. m^{-1}), ρ is the specific resistance of the sample, R is the The resistance and Lis the thickness of the sample.[11,12]

Viscosity

Several key parameters can be calculated using different viscosities, as their values help to elucidate the viscosity variations of the samples. To determine these parameters, specific equations are employed. These equations provide a mathematical framework for understanding the relationships between viscosity and other physical properties of the samples. The relative (η_r), specific(η_{spe}) , reduced (η_{red}), inherent (η_{inh}) and intrinsic [η] viscosities can be calculated using the following equations:[13- 17]

$$\eta_r = \frac{t}{t_s} \quad (4)$$

$$\eta_{spe} = \eta_r - 1 \quad (5)$$

$$\eta_{red} = \frac{\eta_{spe}}{C} \quad (6)$$

$$\eta_{inh} = \frac{\ln \eta_r}{C} \quad (7)$$

$$[\eta] = \frac{(2(\eta_{spe} - \ln \eta_r}{C} \quad (8)$$

Where t_s is the flow time of pure solutions, t is the flow time of solutions and C is the concentration.

Some hydrodynamic parameters

There are several parameters that can be calculated using different viscosities, since their values explain the viscosity variations of the samples. The following equations are used to calculate them: [18]

1- Huggins constant:

$$K_H = \frac{\eta_{red} - [\eta]}{[\eta]^2 C} \quad (9)$$

2- Kraemer constant:

$$K_k = \frac{\eta_{inh} - [\eta]}{[\eta]^2 C} \quad (10)$$

3- Schulz- Blaschks constant:

$$K_{sp} = \frac{\eta_{red} - [\eta]}{[\eta]\eta_{spe}} \quad (11)$$

4- Martin constant:

$$K_M = \frac{\ln \eta_{red} - ln\,[\eta]}{[\eta] C} \quad (12)$$

5- Fuoss constant:

$$K_{Fs} = \frac{\frac{[\eta]}{\eta_{red}} - 1}{C^2} \quad (13)$$

6- polymer parameter concentration:

$$C_{max} = \frac{\eta_r^{0.5} - [\eta]C}{[\eta]} \quad (14)$$

7- Heller constant:

$$K_{He} = -\left(\frac{1}{2}\, C \left(\frac{1}{\eta_{spe}} + \frac{1}{ln \eta_r}\right)\right) - \frac{1}{[\eta]} \quad (15)$$

8- Budtow constant:

$$K_B = 1 - 2K_M \quad (16)$$

9- Arrhenius- Rother- Hoffmorn constant:

$$K_A = \frac{\frac{\ln \eta_r}{C} - [\eta]}{\ln \eta_r} \quad (17)$$

10- Kreisa constant:

$$K_{kr} = \frac{\eta_{spe}^2 (\eta_{red} - [\eta])}{C} \quad (18)$$

11- Staudiuger- Heuer constant:

$$K_{s\text{-}H} = \frac{ln\, \eta_{red} - ln\,[\eta]}{[\eta]\, C} \quad (19)$$

Surface Tension

The surface tension of a solution can be determined using a method that involves measuring the weight of drops. This approach is based on the principle that the surface tension is directly proportional to the weight of the drop and inversely proportional to the circumference of the drop. A specific equation (20) is used to calculate the surface tension, which takes into account the average mass of the drop (m), the acceleration due to gravity (g= 9.8 ms^{-2}) , and the inner radius of the tube used to form the drop. [19].

$$\gamma = \frac{m\, g}{2\, \pi\, r} \quad (20)$$

In this study, the inner radius (r) of the tube was 5 mm, and all measurements were conducted at room temperature, which was maintained at 27°C. Once the surface tension of the solution was determined, additional calculations were performed to evaluate the surface tension force and surface tension energy. These calculations were based on established equations (21) and (22) respectively, that relate the surface tension to the force and energy associated with the surface area of the solution(A) [20- 22].

$$F = 4\, \pi\, r\, \gamma \quad (21)$$

$$E = \gamma\, A \quad (22)$$

Materials and Methods

Materials and Samples preparation

Materials

The materials used in this study included Carboxymethyl cellulose (CMCHV) and Polyanionic cellulose (PAC LV), which were obtained from National Corporation Jowfe Oil Technology. Additionally, Sodium bicarbonate (NaHCO3) was sourced from Foster Clark Products United, a manufacturer based in the European Union, and acetic acid (CH3 COOH) was also used.

Samples preparation

To prepare the samples, carbon dioxide (CO2) was generated through a chemical reaction involving acetic acid and sodium bicarbonate. This reaction follows a specific chemical equation (*), which was used to produce the carbon dioxide used in the study. The resulting carbon dioxide was then utilized in the preparation of the samples, which were used to investigate the properties of CMCHV and PAC LV under various conditions. [23]:

$$NaHCO_{3(s)} + CH_3COOH_{(aq)} \rightarrow CH_3COONa_{(aq)} + H_2O_{(l)} + CO_{2(g)} \quad (*)$$

Where: CH_3COONa = Sodium acetate and H_2O = water

Carbon dioxide was bubbled through double-distilled water to create solutions with varying concentrations of CO2. The resulting solutions had. CO2 concentrations of 27%, 42%, 52%, and 59%. In each of these solutions, either Carboxymethyl cellulose (CMCHV) or Polyanionic cellulose (PACLV) was dissolved at a concentration of 4.5%. This consistent concentration of CMCHV or PACLV allowed for a controlled comparison of the effects of different CO2 concentrations on the properties of these substances.

Measurements

The electrical Properties

Measurements of the electrical properties were conducted by calculating the current density from the electric current intensity measured in the experiment. The potential difference in which the samples were placed was modified to derive the current density. Additionally, the resistance was calculated using Ohm's law, and then the resistivity and conductivity were determined after measuring the height (L) and surface radius (r) of the solutions. The surface area was calculated from these measurements, which was then used to calculate the electric field intensity.

Viscosity

Viscosity measurements were taken using a glass viscometer, which involved measuring the flow time of the samples. The relative viscosity was calculated from this data, and then the specific, reduced, inherent, and intrinsic viscosities were determined. Further calculations were performed to derive various hydrodynamic parameters.

Surface Tension

Surface tension measurements were conducted by dropping a certain weight of solutions and counting the number of drops. The weight of each drop was calculated by dividing the total weight of the solution by the number of drops. The perimeter of each drop was calculated by knowing its radius, and then the surface tension was calculated. The surface tension force and surface tension energy were also calculated from this data.

Results and discussion

The electrical Properties

The results of the electrical properties measurements are presented in a figure (1), which shows the relationship between electric field strength and electric current density for CMCHV/CO2 with varying carbon dioxide concentrations. The electric current density is observed to increase significantly with increasing electric field strength and carbon dioxide concentrations, ranging from a low value (1.89 Am^{-1}) at zero carbon dioxide concentration to a high value (624.56 Am^{-1}) at higher carbon dioxide concentrations.

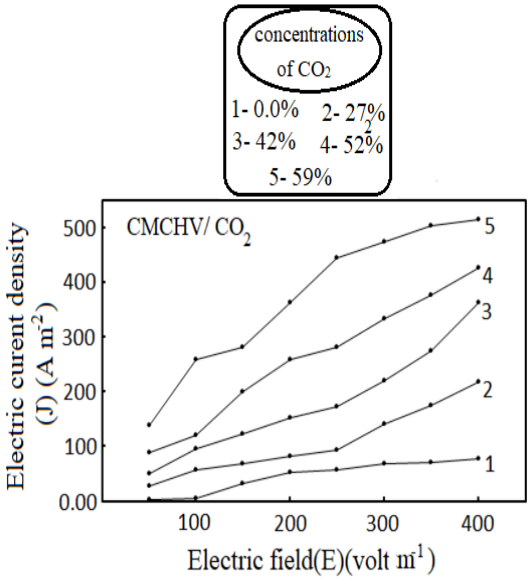

Fig 1. Electric field intensity vs electric current density for CMCHV/CO_2 solutions.

Figure (2) illustrates the relationship between electric field strength and electric current density for PACLV/CO2 with varying carbon dioxide concentrations. The data shows that the electric current density increases from a low value of (1.42 Am^{-1}) at zero carbon dioxide concentration to a higher value of (431.71 Am^{-1}) at higher carbon dioxide concentrations, as the electric field strength and carbon dioxide concentrations increase. A comparison of the data presented in figure (1) and figure (2) reveals that the current density in CMCHV/CO2 solutions exhibits a more significant increase compared to the increase observed in PACLV/CO2 solutions. This suggests that the CMCHV/CO2 solutions are more sensitive to changes in electric field strength and carbon dioxide concentrations, resulting in a greater increase in current density.

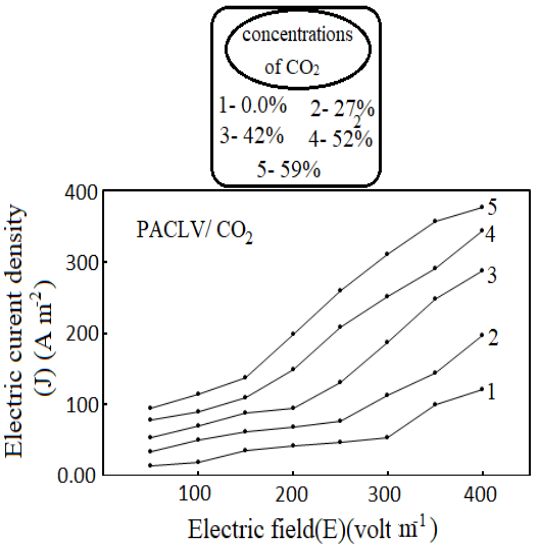

Fig 2. Electric field intensity vs electric current density for PACLV/CO_2 solutions.

Figures (3) and (4) depict the relationship between the square root of the electric field and the logarithm of

the current density for CMCHV/CO2 and PACLV/CO2 solutions, respectively. The logarithm of the current density is indicative of Schottky emission, and the observed relationship demonstrates a direct proportionality between the logarithm of the current density and the square root of the applied electric field. Additionally, the data shows a direct proportionality between the carbon dioxide concentration and the logarithm of the current density. This behavior is characteristic of Schottky emission, which is a phenomenon where the current density increases with the square root of the electric field [24].

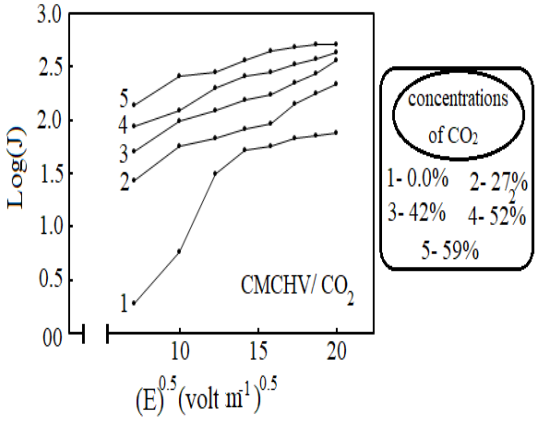

Fig 3. Variation of log (J) with $E^{0.5}$ for CMCHV/CO_2 solutions with different concentrations of CO_2

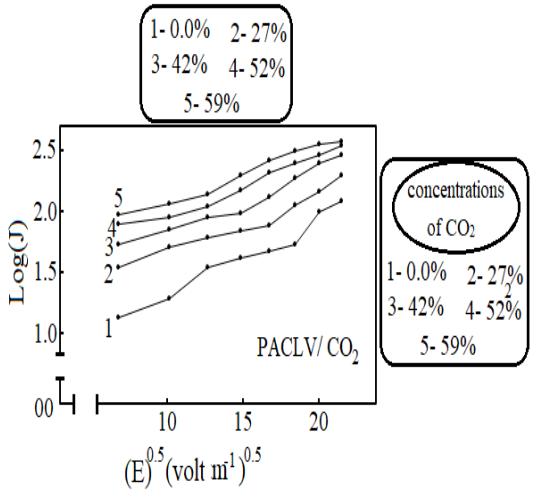

Fig 4. Variation of log (J) with E0.5 for PACLV /CO_2 solutions with different Concentrations of CO_2

The relative viscosity of the solutions is illustrated in fgure (5), which shows the relationship between the relative viscosity and the concentrations of CO2. It is evident that the relative viscosity of both CMCHV/CO2 and PACLV/CO2 solutions increases as the concentration of CO2 increases. For CMCHV/CO2 solutions, the relative viscosity rises from 13.29 at 0% CO2 concentration to 32.53 at 59% CO2 concentration. Similarly, for PACLV/CO2 solutions, the relative viscosity increases from 2.07 at 0% CO2 concentration to 12.09 at 59% CO2 concentration. Notably, the increase in relative viscosity is more pronounced for CMCHV/CO2 solutions compared to PACLV/CO2 solutions, indicating a greater sensitivity to CO2 concentration.

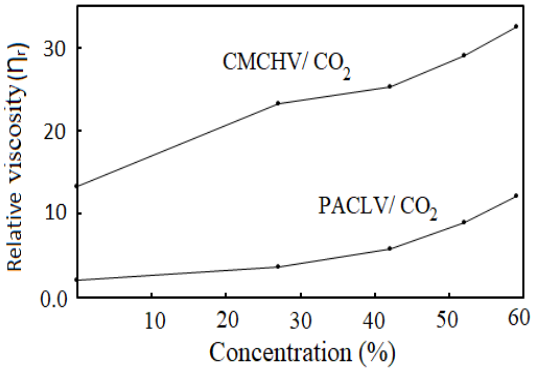

Fig 5. Relative viscosity of the solutions vs the concentrations of CO_2.

The specific viscosity, as illustrated in figure (6), exhibits a similar trend to the relative viscosity of the solutions. The specific viscosity, which is calculated from the relative viscosity, also increases with increasing CO2 concentration. This suggests that the specific viscosity is directly related to the relative viscosity, and that changes in CO2 concentration have a similar effect on both properties. The data in Figure 6 confirms that the specific viscosity follows the same pattern as the relative viscosity, with both properties increasing as the CO2 concentration increases.

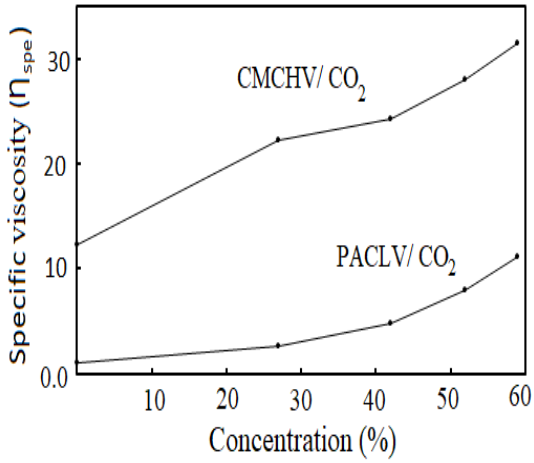

Fig 6. specific viscosity of the solutions vs the concentrations of CO_2.

The reduced viscosity of the solutions exhibits distinct trends in response to increasing CO2 concentrations. In the CMCHV/CO2 solutions, the reduced viscosity decreases as the CO2 concentration increases. In contrast, the reduced viscosity of the PACLV/CO2 solutions increases with rising CO2 concentrations. These opposing trends are evident in the data presented in figure (7). Notably, despite these differences, the reduced viscosity of the CMCHV/CO2 solutions remains higher than that of the PACLV/CO2 solutions across the range of CO2 concentrations.

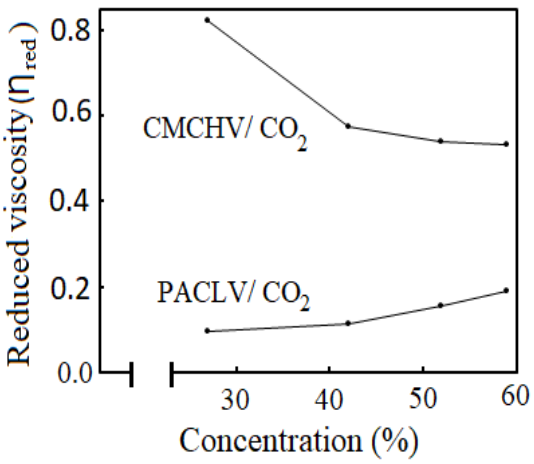

Fig 7. Reduced viscosity of the solutions vs the concentrations of CO_2.

The reduced viscosity exhibits a similar trend in response to changes in specific viscosity, as it does to changes in CO2 concentration. Figure (8) illustrates the relationship between reduced viscosity and specific viscosity, where an increase in reduced viscosity is observed for PACLV/CO2 solutions, while a decrease is noted for CMCHV/CO2 solutions. This mirrors the trend seen in figure (7), where the reduced viscosity changed in response to varying CO2 concentrations. The data suggests that the reduced viscosity is sensitive to changes in both CO2 concentration and specific viscosity, with the PACLV/CO2 solutions exhibiting an increase in reduced viscosity and the CMCHV/CO2 solutions showing a decrease.

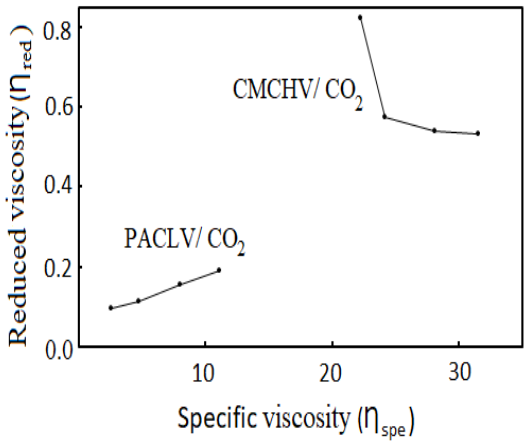

Fig 8. specific viscosity vs reduced viscosity

In figure (9), it is observed that there is a decrease in the inherent viscosities with increasing concentrations of CO_2 in the all samples, but the decrease in inherent viscosities for the PAMLV/ CO_2 samples is less than that for CMCHV/ CO_2.

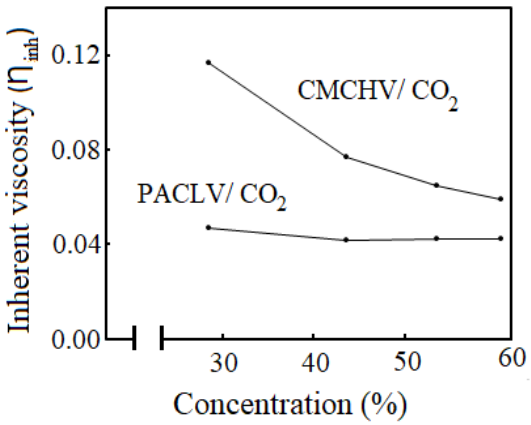

Fig 9. Inherent viscosity of the solutions vs the concentrations of CO_2.

The intrinsic viscosity of the solutions exhibits a decreasing trend with increasing CO2 concentrations. This decrease is observed in both CMCHV/CO2 and PACLV/CO2 solutions. However, the magnitude of the decrease differs between the two types of solutions. The intrinsic viscosity of the CMCHV/CO2 solutions decreases more significantly with increasing CO2 concentrations, whereas the decrease in intrinsic viscosity of the PACLV/CO2 solutions is relatively small. This is evident in the data presented in figure (10), which illustrates the relationship between intrinsic viscosity and CO2 concentration for both types of solutions.

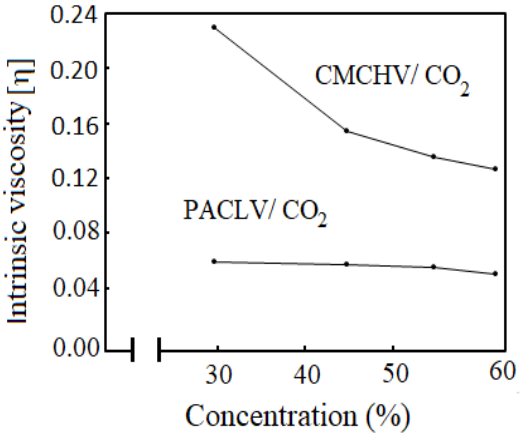

Fig 10. Intrinsic viscosity of the solutions vs the concentrations of CO_2.

Huggins (K_H) and Cramer (K_K) coefficients are criteria for evaluating solvent quality and are calculated from the slope of figure (11) where is calculated from the two equations (9) and (10) respectively and these constants depend on the state of the solution. Huggins (K_H) coefficient values from 0.25 to 0.5 indicate a good solvent and negative K_K values result from good solvents. Table (1) includes Huggins (K_H) and Cramer (K_K) coefficients values for this study [25].

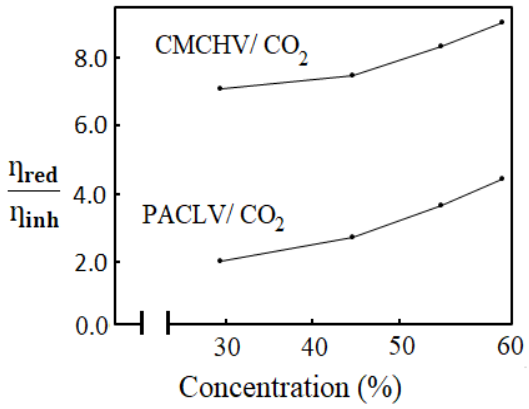

Fig 11. Huggins (KH) and Kramer (Kk) plots for CMCHV/CO_2 and PACLV/CO_2 solutions.[25]

The hydrodynamic parameters of the polymer chains used in this study indicate that they are flexible in nature. The values of these parameters range from (0.369) to (0.923) for the PACLV/CO2 samples and from (0.42) to (0.49) for the CMCHV/CO2 samples, as shown in Tables (1) and (2) [26]. Table 1 provides the values of the coefficients calculated using equations (9) to (19), which can also be determined from the slope of the plots connecting the variables in these equations. These calculations provide insight into the behavior of the polymer chains in the presence of CO2 [18].

Table (1) some hydrodynamic parameters values for the CMCHV.

Constants	CMCHC/CO_2			
	Concentration (%)			
	27	42	52	59
K_H	0.421	0.423	0.426	0.429
K_k	-0.079	-0.078	-0.074	-0.071
K_{spe}	0.211623	0.122885	0.120705	0.114261
K_M	0.046	-0.262	-0.331	-0.351
K_{Fs}	-0.001	-0.00042	-0.00028	-0.00022
C_{max}	15.45	17.21	22.26	24.39
K_{He}	-0.53	-0.891	-1.244	-1.53
K_B	0.908	1.525	1.661	1.702
K_A	-0.036	-0.024	-0.021	-0.0195
K_{kr}	0.492	0.243	0.2197	0.218
K_{S-H}	0.207	0.204	0.197	0.192

Table (2) some hydrodynamic parameters values for the PACLV.

Constants	PACLV/CO_2			
	Concentration (%)			
	27	42	52	59
K_H	0.369	0.404	0.614	0.923
K_k	-0.131	-0.114	-0.083	-0.054
K_{spe}	0.553	0.383	0.372	0.343
K_M	-0.596	-0.992	-0.870	-0.664
K_{Fs}	-0.0005	-0.0003	-0.0003	-0.0002
C_{max}	38.68	53.55	62.96	70.26
K_{He}	0.906	1.012	2.935	5.391
K_B	2.192	2.985	2.741	2.327
K_A	-0.017	-0.009	-0.006	-0.003
K_{kr}	0.003	0.006	0.015	0.026
K_{S-H}	0.290	0.282	0.353	0.444

Concentration is a crucial parameter (C^*) that significantly influences the properties of a solution, particularly in the presence of an external field. As the concentration of a polymer solution increases, the spacing between molecular segments changes, affecting the solution's properties, film structure, and device performance. Polymer solutions can be broadly categorized into two groups: dilute and concentrated solutions. A gradual increase in concentration from dilute to concentrated can lead to a transformation in the properties of the molecular condensed state [27].

Surface Tension

The surface tension of the samples was calculated using equation (20) and plotted in figure (12). The results show that the surface tension increases with increasing carbon dioxide concentrations for both samples. However, the increase in surface tension is more pronounced for CMCHV/CO2 compared to PACLV/CO2. This suggests that the addition of carbon dioxide has a greater impact on the surface tension of CMCHV/CO2 solutions, potentially affecting their behavior and properties.

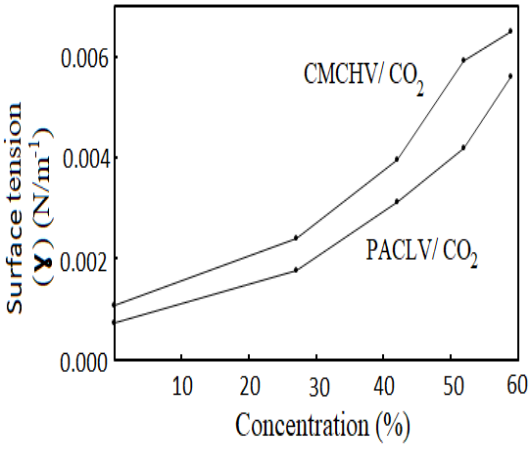

Fig 12. Surface tension vs concentration of CO_2.

The surface tension force and energy were calculated using equations (21) and (22), respectively. The results are presented in figures (13) and (14), which show that both the surface tension force and energy

increase with increasing CO2 concentration. This indicates a direct relationship between the CO2 concentration and the surface tension properties of the solutions. As the CO2 concentration increases, the surface tension force and energy also increase, suggesting that the addition of CO2 has a significant impact on the interfacial properties of the solutions.

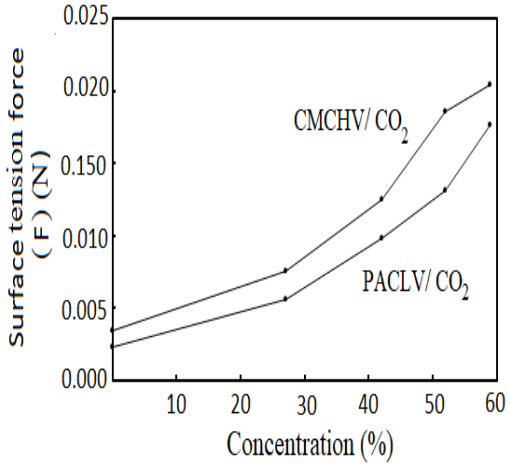

Fig 13. Surface tension force vs concentration of CO_2

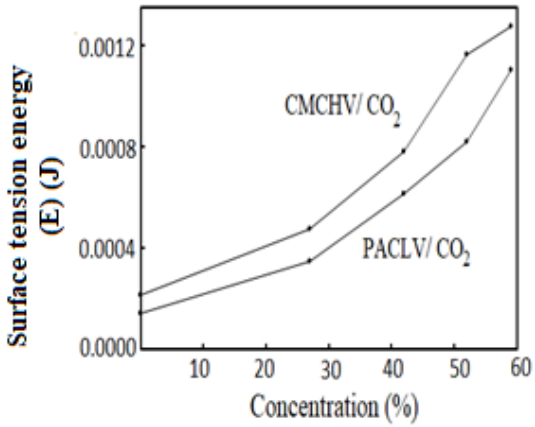

Fig 14. Surface tension energy vs concentration of CO_2

Conclusion

The results of this study show that changing the concentrations of carbon dioxide in the solutions of CMCHV and PACLV caused their conductivity, viscosity, and surface tension to change, all of which increased to varying degrees. This indicates that carbon dioxide in the atmosphere when dissolved in water used to extract oil in oil fields and wells causes the physical properties of CMCHV and PACLV to change because they are used in solid-laden and water-based drilling fluids, which can effectively reduce the filtration rate of many water-based drilling fluids, and it is preferable that their viscosity is low [28]. This study can be used to change the physical properties, especially the viscosity of CMCHV and PACLV to avoid the effect of carbon dioxide on them.

Acknowledgment

I would like to thank National Oil Corporation Jowfe Oil Techonlogy that supplied me with the polymers, especially Mr. Mohammad Bograd, and Mr. Jamal Mohammad Al-Farjani.

References

[1] M. Santoro, F. A. Gorelli, K. Dziubek, D. Scelta, and R. Bini," Structural and Chemical Modifications of Carbon Dioxide on Transport to the Deep Earth", the American Geophysical Union and John Wiley and Sons, 2020.

[2] T. Kar and A. Firoozabadi," Effective viscosification of supercritical carbon dioxide by oligomers of 1-decene", iScience 25, 104266, 2022.

[3] B. Metz, O. Davidson, H. de Coninck M. Loos and L. Meyer," IPCC Special Report on Carbondioxide capture and storage", Cambridge University Press, Published for the Intergovernmental Panel on Climate Change, 2005.

[4] M. S. Rahman , M. S. Hasan , A. S. Nitai , S. Nam, A. K. Karmakar, M. S. Ahsan, M.J. A. Shiddiky and M. B. Ahmed ," Recent Developments of Carboxymethyl Cellulose", Polymers, , 13, 1345, 2021.

[5] H. Rasheed, A. Adeleke, P. Nzerem, Olusegun Ajayi, Peter Ikubanni, Asmau Mana," A review on the use of carboxymethyl cellulose in oil and gas fifield operations", pringer Nature B.V, 30, 9899–9924, 2023.

[6] A. Busch, V. Myrseth, M. Khatibi, P. Skjetne, S. Hovda, S. T. Johansen," Rheological Characterization of Polyanionic Cellulose Solutions with Application to Drilling Fluids and Cuttings Transport Modeling", Applied Rheology, 28, 25154, 2018.

[7] Liao et al," Experiments: (2) Faraday Ice Pail Topic Introduction", Topics: Capacitors Related Reading: Course Notes, Sections 4.3-4.4; Chapter 5.

[8] R. G. Rastogi," Conductivity, electric field and electron drift velocity within the equatorial electrojet", Earth Planets Space, 58, 1071–1077, 2006.

[9] J. L. Davidson , C.J.D. Pomfrett and H. McCann," Predicted EIT current densities in the brain using a 3D anatomically realistic model of the head", Springer,IFMBE Proceedings Vol. 17, pp. 376–379, 2007.

[10] S. Hughes," Lecture 7: Current, continuity equation, resistance, Ohm's law", Massachusetts Institute of Technology Department of Physics,2005.

[11] E. R. R. Solórzano, S. J. M. León, R. C.Legoas, Y. A. C.Juanito, G. R. .Uchamaco, A. F. T.Arroyo and E. M.Contreras," Variation of the Electrical Resistivity of Peruvian Tropical Woods", Floresta Ambient., Rio de Janeiro, 31, 2179-8087, 2024.

[12] A. A. Bery, N. el H. Ismail," Empirical correlation between electrical resistivity and engineering properties of soils", Soil Mechanics and Foundation Engineering, 54, 6, 2018. DOI 10.1007/s11204-018-9491-7

[13] S. T. S.-Abadi, S. M. A. Razavi , M. Irani, " Intrinsic Viscosity and Molecular Parameters of Wheat Starch-Cress Seed Gum-Sucrose Mixture", Biointerface research in applied chemistry, 11, 12068 – 12081, 2021.

[14] M.A.Taha, V. B.Legaré, F. N. de Andrade, R. L. D. Rosario, T. Mckenna, R. Fulchiron," Determination of viscosity average molar masses of polyethylene in a wide range using rheological measurements with a harmless solvent", HAL Id: hal, 03296436, 2021.

[15] J. C. Rauschkolb, B. C. Ribeiro, T. Feiden, B. Fischer, T. A. Weschenfelder, R. L. Cansian, A. Junges," Parameter Estimation of Mark-Houwink Equation of Polyethylene Glycol (PEG) Using Molecular Mass and Intrinsic Viscosity in Water", Biointerface Research in Applied Chemistry, vol. 12, 2022.

[16] A. E. Yarawsky, V. Dinu, S. E. Harding and A. B. Herr**,"** Strong non-ideality effects at low protein concentrations: considerations for elongated proteins**",** Eur Biophys J, 52, 2023.

[17] B. C. C. D. Cunha, M. G. Domingues and J. A. F. Rocco," A viscometric study of mixtures with hydroxyl-terminated polybutadiene (HTPB) and short chain diols used in the formulations of solid composite propellants", Chemical Sciences, 93, 2021.

[18] M. A. Masuelli, " Intrinsic Viscosity Determination of High Molecular Weight Biopolymers by Different Plot Methods. Chia Gum Case", Journal of Polymer and Biopolymer Physics Chemistry, 6, 13-25 2018.

[19] M. Soni," A simple laboratory experiment to measure the surface tension of a liquid in contact with air", Journal of Pharmacognosy and Phytochemistry, 8, 2197-2202, 2019.

[20] A. Garcia, T. Dessev, L. Guihard, S. S. Chevallier, M. Havet, A. L.Bail," Impact of external static electric field on surface tension of model solutions", HAL Id: hal-04147599, 2023

[21] G. Clément, G. Axe, J. Léa," Generation and trajectory control of water drops able to bounce on a flat water surface*,"* Emergent Scientist, 1, 2017.

[22] L. Ruan, J. Liu, S. Sueda, B. Wang, B. Chen," Solid-Fluid Interaction with Surface-Tension-Dominant Contact", ACM Trans. Graph, 40, 2021.

[23] K. W. Omari, and J, B. Mandumpal," A simple pedagogical limiting reactant kitchenette experiment including a simple algorithm", Chemistry Teacher International 5, 75–81,2023

[24] X. G. Tang, et al.," Leakage current and relaxation characteristics of highlyÑ111Ö-oriented leadcalcium titanate thin films", Journal of Applied Physics, American Institute of Physics, 94, 2003.

[25] N. A. Elgheryani," Effect of Changing the Concentration of Zinc Oxide Nanoparticles on the Viscosity of the Polyacrylamide / Polyethylene Glycol Solutions", Libyan Journal of Basic Sciences (LJBS) 16, 90- 100 , ,2707-6261,2022.

[26] R, Pamies, J. G. H. Cifre · M. d. C. L. Martínez, José García de la Torre," Determination of intrinsic viscosities of macromolecules and nanoparticles. Comparison of single-point and dilution procedures", Colloid Polym Sci, 286,1223–1231,2008.

[27] Y. Zhang, D. Cheng, T. Li, Y. Guan, B. Liu, H. Zhang,| D. Lu," Concentration effect on the chain structure and photoelectric properties of conjugated polymer precursor solutions and thin films: A mini review," Journal of polymer science, 62, 1156–1174, 2023.

[28] P. Talukdar, S. B.Gogoi," A Study on the role of Polyanionic Cellulose (PAC) in the ndde for the oilfields of Upper Assam Basin", International Journal of Engineering Research &) Technology, 4, 2015.